

# FACTORS CONTRIBUTING TO R-CURVE BEHAVIOUR IN ZIRCONIA CERAMICS

M. V. Swain and R. H. J. Hannink

*Advanced Materials Laboratory, CSIRO Division of Materials Science, Melbourne, Victoria, Australia*

## ABSTRACT

Three distinct types of microstructures have been found to develop R-curve behaviour in zirconia ceramics. These include materials where: a transformation process zone forms about the crack tip in partially stabilized zirconia (PSZ) containing metastable tetragonal precipitates, microcracking/crack branching occurs in decomposed monoclinic zirconia, and crack deflection by coarse monoclinic precipitates in overaged PSZ materials. Of these the greatest toughening increment occurs where a transformation process zone forms about the crack tip. This R-curve behaviour is accompanied by "plastic" like behaviour during the initial crack loading of a brittle ceramic. Examples of the R-curves for PSZ materials containing metastable tetragonal precipitates and microcracking in decomposed monoclinic zirconia are presented. Also substantial differences are found between K and J approaches for determining the R-curve.

## INTRODUCTION

At the previous conference of this series (ICF5) it was revealed that partially stabilized zirconia (PSZ) ceramics typically possess  $K_{Ic}$  values twice that of other engineering ceramics (Swain and Hannink, 1981). PSZ ceramics are usually prepared such that a large fraction of precipitates of the metastable tetragonal phase of zirconia are formed in the cubic zirconia matrix during cooling or heat treatment. These tetragonal precipitates can be transformed to the low temperature stable monoclinic phase of zirconia by the application of stress. Such a transformation is generally considered martensitic and is accompanied by a volume dilation which reduces the tensile stress field about the crack tip (Garvie, Hannink and Pascoe, 1975; Porter and Heuer, 1977; Dworak, Olapinski and Thamerus, 1977).

In some ways PSZ ceramics are analogous to trip steels. As early as 1968 Antolovich recognized the possibility of R-curve behaviour developing in these steels as a consequence of the transformation process. More recently a number of theoretical treatments dealing more exclusively with transformation toughening in PSZ ceramics have predicted R-curve behaviour (Marshall, Evans and Drory, 1983; McMeeking and Evans, 1982; Rose, 1984).



Observations of R-curve behaviour in strong ceramics ( $MOR > 500 \text{ MPa}$ ) have been limited. Recent studies investigating the grain size dependence of the fracture toughness of alumina (Mussler, Swain and Claussen, 1982; Steinbrech, Khehans and Schwaarwachter, 1982) revealed increasing R-curve behaviour with increasing grain size. Studies of PSZ materials have shown that this material exhibits considerable R-curve behaviour. Green, Nicholson and Embury (1973) found that in calcia-PSZ (Ca-PSZ) R-curve behaviour was associated with cracking at grain boundaries adjacent to the main crack tip. This material had very low strength and relatively low fracture toughness. More recently Swain (1983) presented evidence for profound R-curve behaviour in magnesia-PSZ (Mg-PSZ) particularly after "sub-eutectoid" heat treatment. This occurred in materials with high strength ( $> 600 \text{ MPa}$ ) and high fracture toughness ( $> 500 \text{ J/m}^2$ ). However, these latter observations suggested the rise in toughness with crack extension occurred over distances as large as  $500 \mu\text{m}$ . It was found that the resistance to strength degradation resulting from thermal shock was also much greater in these materials.

In this paper only materials with transformation toughening and microcracking induced R-curve behaviour will be considered. More detailed aspects of the microstructural features of these and other PSZ materials exhibiting R-curve behaviour are presented elsewhere (Swain and Hannink, 1984).

#### MATERIAL SELECTION AND TESTING ARRANGEMENT

Whilst R-curve behaviour has been observed in PSZ materials using both calcia and magnesia stabilisers, the present work will concentrate on Mg-PSZ exclusively because of the more profound R-curve effects observed in this material. Previous work also indicated that certain heat treatments imparted greater R-curve behaviour than others (Swain, Hannink and Garvie, 1983b). This was identified by high stability of the fracture process during single edged notched beam (SENB) tests. It was found that the total energy demand to fracture a notched bar could be up to three times the energy to initiate crack extension. Such phenomena had been reported for refractory bricks and some rocks but not for strong ceramics.

The results presented here will concentrate on two Mg-PSZ materials of the same composition, containing 9.5 mol% MgO and the remainder zirconia, fired at  $\sim 1700^\circ\text{C}$  then cooled in a very controlled manner. One material had highly metastable tetragonal precipitates on cooling, the other was 'sub-eutectoid' heat treated at  $1100^\circ\text{C}$  to develop a continuous thick ( $\sim 5\text{--}10 \mu\text{m}$ ) monoclinic zirconia phase at the grain boundaries. The latter material also contained precipitates which transformed to monoclinic on cooling as a consequence of the heat treatment.

Fracture tests were carried out using the SENB test in a highly instrumented rig. Complementary observations were made using the double cantilever technique (DCB). The latter tests were performed on relatively large plates ( $30 \times 80 \times 4 \text{ mm}$ ) containing a shallow groove  $\sim 0.5 \text{ mm}$  machined on each side. A starting notch  $\sim 10\text{--}15 \text{ mm}$  beyond the loading points was also introduced. All specimens were subsequently annealed at  $\sim 1000^\circ\text{C}$  for 15 minutes prior to testing to remove surface compressive stresses introduced by machining (Swain, Hannink and Garvie, 1983b). The specimen was loaded in a "stiff" machine at slow cross head speeds ( $0.05 \text{ mm/min}$ ) in air or kerosene (the latter to reduce stress corrosion effects). Crack extension was generally very stable, particularly for high toughness materials, and was monitored either directly, with dye penetrant or load line compliance.

After DCB testing the arms of the fractured specimen were notched with a

$100 \mu\text{m}$  diamond saw blade to at least 0.5 of the specimen section for NB testing after a similar anneal treatment. NB tests were performed in a 3-point bend arrangement with a moment arm of  $20 \text{ mm}$  at a crosshead displacement of  $0.05 \text{ mm/min}$ . Compliance of the specimen was monitored with a very sensitive linear variable displacement transducer (LVDT) between loading platten and load cell. It has been found that the NB test is more sensitive than the DCB technique for monitoring R-curve behaviour as small changes in crack growth are readily measurable by changes in compliance. An acoustic emission (AE) detector was attached to some specimens during fracture testing.

#### OBSERVATIONS AND DISCUSSION

As outlined above the present observations were limited to materials representing only two mechanisms responsible for R-curve behaviour. However, other materials with a range of properties between these two may be developed by suitable modifications including firing temperature, composition and heat treatment.

##### (i) Transformation Toughened (TT) PSZ Materials

A typical observation of the force displacement curve for TT-Mg-PSZ when SENB tested is shown in Fig. 1. It is usually found that a distinct break in the normal loading curve occurs well before peak load is achieved. Also shown in Fig. 1 is the total accumulated counts from an acoustic emission detector. The point of onset of detectable noise coincides with the break from the loading curve. However, rapid accumulation of counts only occurs after peak load has been achieved.

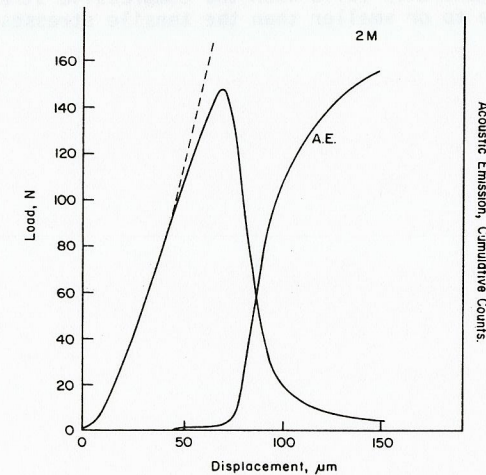


Fig. 1. Force-displacement curve generated during SENB testing of a transformation toughened Mg-PSZ material. Also shown is the accumulated acoustic emission signal during the fracture test.

Analysis of the results in Fig. 1 would usually proceed by determining secant



compliance at various points on the load displacement curve after subtracting the test rig compliance. Then, using either computed or experimentally determined compliance-crack length relationship, stress intensity factor with crack extension may be determined. For cracks deeper than 0.6 of specimen section  $K_{1c}$  values were evaluated using the expression developed by Wilson (1970). However, this whole approach leads to an erroneous R-curve for the material.

The error in such an approach is readily appreciated by comparing the observations in Fig. 1 with those generated in Fig. 2. Complete unloading of the specimen was made at various stages of the loading curve in the latter case. This enabled the compliance at various stages of crack extension to be determined so that precise estimates of crack propagation could be made.

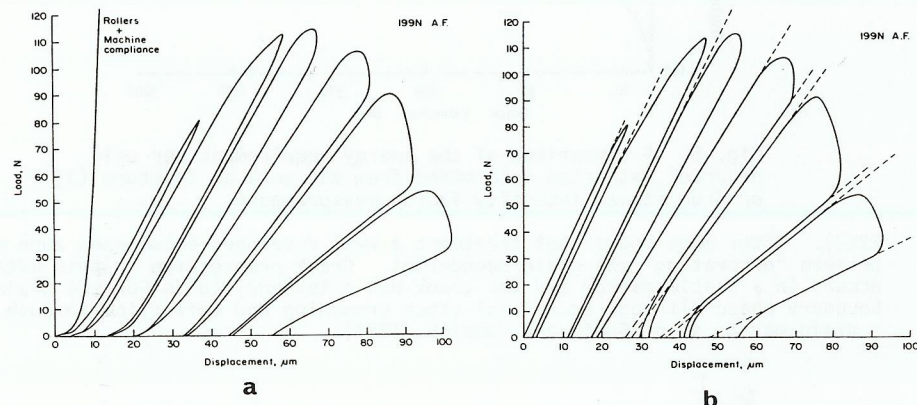


Fig. 2. Force-displacement curve for transformation toughened Mg-PSZ with unloading at various stages during the SENB test. (a) Raw data, and (b) upon removal of machine and testing rig compliance. A small offset was introduced between unloading and reloading for both curves.

It is obvious from Figs. 2(a) and (b) that substantial residual crack opening displacement occurs even prior to the achievement of the peak load and that little change in compliance has occurred despite the "plastic" like behaviour of the specimen. Observations revealed that some grains adjacent to the crack tip were deformed by twinning and that considerable uplift of material adjacent to the crack occurred. This uplift was greatest near the crack tip, as would be anticipated for a material showing transformation toughening. Another feature of the compliance curves was the deflection from linearity during the initial stages of loading and unloading, supporting the notion of an expanded zone about the crack tip preventing crack closure.

Analysis of the results in Fig. 2 are shown in Fig. 3 for notches of different depths on similar sized specimens. The paucity of results on the steeply rising section of the R-curve reflects the difficulty of manually unloading the specimen during the initial section of the loading curve. The rise in toughness occurs over a crack extension of some  $\sim 50\mu\text{m}$ , thereafter the slope of the R-curve decreases dramatically becoming almost horizontal. The maximum value approaches the steady stage DCB value for the toughness. Observations of the crack initiation region of the SENB fracture test revealed no major difference from the remainder of the stably propagated fracture

surface. In general, the fracture morphology appeared very tortuous and at high magnification SEM observations indicated that the crack path had deviated about precipitates.

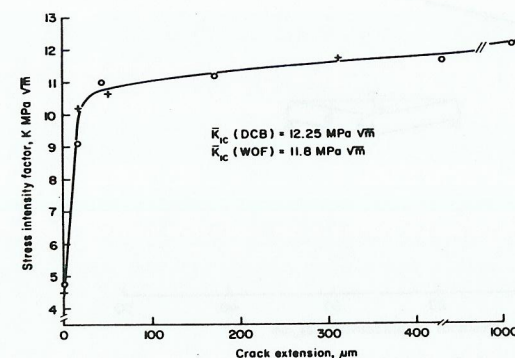


Fig. 3. Calculated R-curve from the results in Fig. 2.

The material tested contained highly metastable tetragonal precipitates; heat treatment for one hour at  $1100^\circ\text{C}$  was sufficient to destabilise all the tetragonal precipitates so that on cooling they transformed to monoclinic zirconia. The fracture toughness of such a material was greatly reduced, SENB and DCB tests gave comparable values of  $K_{1c} = 4.4 \pm 2 \text{ MPa}\sqrt{\text{m}}$  and showed virtually no evidence of R-curve behaviour.

Theoretical predictions of R-curve behaviour in PSZ materials (Marshall, Evans and Drory, 1983; McMeeking and Evans, 1982) suggest that the steep rise in toughness should occur over a crack extension of between one and two times the transformed zone size and asymptotically approach a limiting value. The results in Fig. 3 would agree with predictions if the zone size was  $\sim 20\text{--}30\mu\text{m}$ . This is a very large zone size, almost an order of magnitude greater than previously observed in PSZ systems (Swain, Hannink and Garvie, 1983b). An estimate may be inferred from observations of the uplifted zone about the crack tip, this gave a value of  $\sim 20\text{--}25\mu\text{m}$  (Swain and Hannink, 1984). Another method is to calculate the zone size from the measured increase in  $K_{1c}$  from theoretical expressions (McMeeking and Evans, 1982), namely

$$\Delta K_{1c} = 0.22 V_f e^T E \sqrt{h} / (1 - \nu^2) \quad (1)$$

where  $\Delta K_{1c}$  is the transformation toughening increment,  $e^T$  the unconstrained dilatational transformation strain,  $E$  Young's modulus,  $\nu$  Poisson's ratio,  $V_f$  is the volume fraction of transformable tetragonal precipitates, and  $h$  is the width of the transformation zone. Substituting the following values,  $V_f = 0.4$ ,  $e^T = 0.06$ ,  $E = 205 \text{ GPa}$ ,  $\nu = 0.25$ , and  $\Delta K_{1c} = 7.6 \text{ MPa}\sqrt{\text{m}}$  in equation (1) gives a value of  $h = 23\mu\text{m}$ . Both estimates of  $h$  are in good agreement with the predictions of Marshall et al (1983).

The feature of the present results that has not been considered in theoretical treatments published to date is the significance and extent of permanent offset. This aspect is shown in more detail in Fig. 4, and closely follows the R-curve behaviour of the material. The permanent offset appears to initiate at a specific  $K$  or  $J$  value and then follows the rate of change of  $J$  with crack extension. Such a relationship was proposed by Rice and Sorenson (1978)



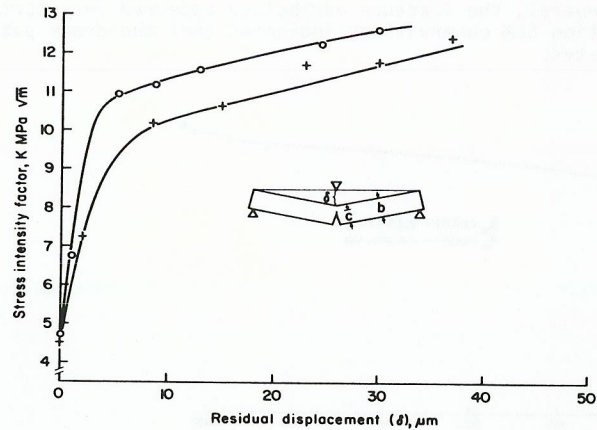


Fig. 4. Permanent 'plastic' like offset of Mg-PSZ versus nominal stress intensity factor when SENB tested.

for elastic-plastic materials and has since been advocated by Smith (1983) for brittle materials that undergo extensive microcracking. A more complete discussion of this permanent plastic deformation in PSZ ceramics will be presented at a later date (Rose and Swain, 1984).

Another aspect of the results presented in Fig. 2 is that they may be interpreted in terms of a work of fracture or  $J$ . This involves determining the energy absorbed for each increment of crack extension. The area under the load-unload cycle is a measure of the energy absorbed and the change in compliance indicates the crack extension per cycle. To enable comparison the  $K$  results in Fig. 3 have been converted to  $G$  following the normal convention and both approaches are plotted in Fig. 5. This figure shows that there is a substantial difference between the two methods, particularly during first few hundred microns of crack extension. However, after some 300  $\mu\text{m}$  of crack extension the two approaches converge. The work of fracture ( $J$ ) is initially much higher than  $G$  determined from stress intensity measurements. Such a difference has recently been predicted by Rose (1984) and will be discussed in more detail by Rose and Swain (1984). However, the physical significance of the results is that the work of fracture measures external work supplied to the system which is absorbed in the generation of the transformed zone in front of the crack tip. Whereas the stress intensity factor indicates the effect of internal stresses on the crack tip, the significance of the latter stresses is greatest when they operate on the wake of the crack.

#### (ii) PSZ Materials with Microcracking Induced R-Curves

The materials referred to here contain relatively large amounts of continuous monoclinic phase usually formed by sub-eutectoid heat treatment which decomposes the matrix. As discussed elsewhere (Swain, Garvie and Hannink, 1983a) magnesia fully stabilized zirconia (Mg-CSZ) displays considerable R-curve behaviour upon partial or fully decomposing to monoclinic zirconia.

The decomposition reaction in Mg-PSZ initiates at grain boundaries and also leads to destabilization of the tetragonal precipitates (Hannink and Garvie,

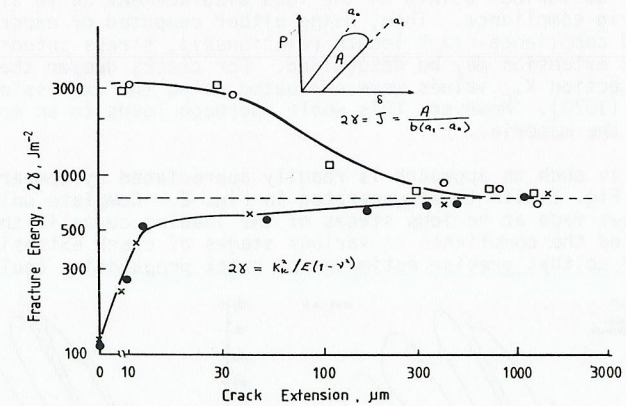


Fig. 5. A comparison of the energy requirement per unit of crack extension determined from the work or fracture ( $J$ ) or from stress intensity factor measurements.

1982). After many hours heat treatment a well developed decomposed zone may be seen "decorating" the grain boundaries. Crack propagation in this material occurs in a stable manner and the crack has a tendency to follow the grain boundary phase although occasional crack branching and deflection through a grain may be seen (Swain and Hannink, 1984).

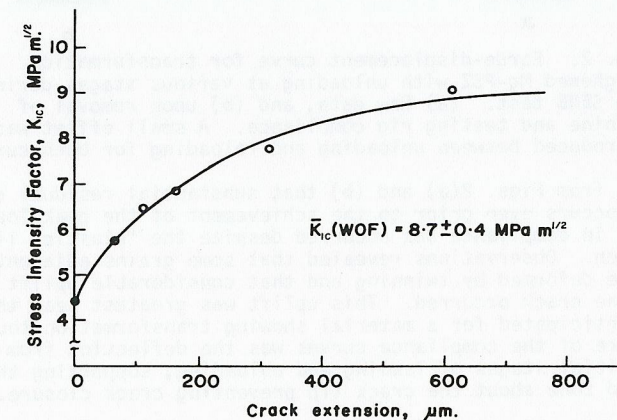


Fig. 6. R-curve for the material containing monoclinic zirconia at the grain boundary.

The R-curve in such a material is shown in Fig. 6. The rate of change is substantially different from TT-PSZ materials (Fig. 3). The other differences are the absence of the large initial offset observed with TT materials and no obvious uplift about the crack. However, permanent offset does occur,



the extent of which again follows the rise in K with crack extension. These observations agree with those of Wnuk and Mura (1981) who observed similar behaviour during the testing of granite rocks. Scanning and transmission electron microscope observations (Swain and Hannink, 1984; Swain, Garvie and Hannink, 1983a) of a crack passing through the grain boundary phase reveal substantial microcracking. The zone of the microcracking was almost the complete width of the decomposed zone size and on a fine scale microcracking occurred where the crack interacted with MgO rich pipes formed during the decomposition reaction. The spacing of the latter features was less than 0.5 $\mu$ m, leading to a relatively severely microcracked material. As pointed out for Mg-CSZ materials (Swain, Garvie and Hannink, 1983a), residual thermal expansion anisotropy (TEA) stresses are probably contributing significantly to the development of microcracking in the monoclinic phase. In addition the lower thermal expansion of the monoclinic than the PSZ phase would lead to tensile stresses developing and fracture occurring within the grain boundary.

#### CONCLUSIONS

Evidence of R-curve behaviour in Mg-PSZ materials with two completely different microstructures and by different mechanisms has been presented. The toughness increment was much greater in materials displaying transformation toughening than material generating microcracking about the crack tip. The R-curve effect occurred over a shorter crack extension in TT material than microcracked material, the former also agreed with theoretical predictions. Permanent offset effects occurred with both materials but were more profound during the initial stages of crack extension in TT materials.

#### REFERENCES

- Antolovich, S.D. (1968). *Trans. AIME*, **242**, 2371-2373.
- Dworak, U., H. Olapinski and G. Thamerus (1977). *Sci. of Ceram.*, **9**, 543-550.
- Garvie, R.C., R.H.J. Hannink and R.T. Pascoe (1975). *Nature*, **258**, 703-705.
- Green, D.J., P.S. Nicholson and J.D. Embury (1973). *J. Am. Ceram. Soc.*, **56**, 619-623.
- Hannink, R.H.J. and R.C. Garvie (1982). *J. Mater. Sci.*, **17**, 2637-2644.
- Marshall, D.B., A.G. Evans and M.D. Drory (1983). *Fracture Mechanics of Ceramics*, **6**, 289-308. Plenum Press.
- McMeeking, R. and A.G. Evans (1982). *J. Am. Ceram. Soc.*, **65**, 242-245.
- Mussler, B., M.V. Swain and N. Claussen (1982). *J. Am. Ceram. Soc.*, **65**, 566-572.
- Porter, D.L. and A.H. Heuer (1977). *J. Am. Ceram. Soc.*, **60**, 183-184.
- Rice, J.R. and E.P. Sorenson (1978). *J. Mech. Phys. Sol.*, **26**, 163-169.
- Rose, L.R.F. (1984). Unpublished work.
- Rose, L.R.F. and M.V. Swain (1984). To be published.
- Steinbrech, R., R. Khehans and W. Schwaarwachter (1982). *J. Mater. Sci.*, **18**, 265-270.
- Smith, E. (1983). *J. Mater. Sci. Lett.*, **2**, 204-206.
- Swain, M.V. and R.H.J. Hannink (1981). *ICFS, Adv. in Fract. Res.*, **4**, 1559-1567.
- Swain, M.V., R.C. Garvie and R.H.J. Hannink (1983a). *J. Am. Ceram. Soc.*, **66**, 358-362.
- Swain, M.V., R.H.J. Hannink and R.C. Garvie (1983b). *Fracture Mechanics of Ceramics*, **6**, 339-354. Plenum Press.
- Swain, M.V. (1983). *Fracture Mechanics of Ceramics*, **6**, 355-369. Plenum Press.
- Swain, M.V. and R.H.J. Hannink (1984). *Advances of Ceramics*, Vol. 12, to be published (Am. Ceram. Soc.).
- Wilson, W.K. (1970). *Eng. Fract. Mechs.*, **2**, 169-171.
- Wnuk, W.P. and T. Mura (1981). *Int. J. Fract.*, **17**, 493-507.